

Three-Mirror Anastigmat Telescope with an Unvignetted Flat Focal Plane

Kyoji NARIAI

Department of Physics, Meisei University, Hino, Tokyo 191-8506

nariai.kyoji@gakushikai.jp

and

Masanori IYE

Optical and Infrared Astronomy Division, National Astronomical Observatory, Mitaka, Tokyo 181-8588

iy@optik.mtk.nao.ac.jp

(Received 2004 September 1; accepted 2004 December 17)

Abstract

A new optical design concept of telescopes to provide an aberration-free, wide field, unvignetted flat focal plane is described. The system employs three aspheric mirrors to remove aberrations, and provides a semi-circular field of view with minimum vignetting. The third mirror reimages the intermediate image made by the first two-mirror system with a magnification factor on the order of unity. The present system contrasts with the Korsch system where the magnification factor of the third mirror is usually much larger than unity. Two separate optical trains can be deployed to cover the entire circular field, if necessary.

Key words: Telescopes

1. Introduction

Most of the currently used reflecting telescopes are essentially two-mirror systems where major Seidel aberrations of the third order are removed, but not entirely. The addition of a third aspheric mirror to construct telescope optics enables the removal of remaining major aberrations (Paul 1935; Robb 1978; Yamashita, Nariai 1983; Epps 1983; Schroeder 1987; Wilson 1996). For instance, Willstrop (1984) designed a wide-field telescope with three aspheric mirrors, giving 4° field of view with an image size better than $0''.31$, or a 3° field of view with a flat focal plane (Willstrop 1985). Rakich and Rumsey (2002) as well as Rakich (2002) found solutions for a flat-field three-mirror telescope with only one mirror aspherized. However, many of the three-mirror telescope designs suffer from obscurations, except for the design reported by Korsch (1980) for practical applications. A four-mirror telescope with spherical primary is another approach to

achieve small obstruction (Meinel et al. 1984; Wilson et al. 1994; Rakich, Rumsey 2004). In the present paper, we report on a new concept of three-mirror telescope design for a next-generation extremely large telescope.

2. Two-Mirror System

An all-mirror optical system is characterized by the set of the aperture \mathcal{D}_i , the radius of curvature r_i , and the distance to the next surface of the i -th mirror surface d_i . We use \mathcal{D}_1 to represent the aperture diameter of the primary mirror.

The geometry of a two-mirror system is determined when four design parameters (\mathcal{D}_1 , r_1 , d_1 , r_2) are given. We adopt a coordinate system where light proceeds from left to right. Thus, in a two-mirror system, $r_1 < 0$ and $d_1 < 0$; while $r_2 < 0$ for a Cassegrain system and $r_2 > 0$ for a Gregorian system.

Instead of radius r , we can also use focal length f . In this case, f is positive for a concave mirror and is negative for a convex mirror:

$$f_1 = -\frac{r_1}{2}, \quad f_2 = \frac{r_2}{2}. \quad (1)$$

We represent the distance from the second mirror to the focal plane of the two-mirror system by d_2 . The imaging formula for the secondary mirror gives

$$\frac{1}{-(f_1 + d_1)} + \frac{1}{d_2} = \frac{1}{f_2}, \quad (2)$$

and the geometrical relation gives the ratio of focal lengths,

$$\frac{f_1}{f_{\text{comp}}} = \frac{f_1 + d_1}{d_2}, \quad (3)$$

where f_{comp} is the focal length of the composite system.

For a two-mirror system, instead of d_2 , we often use the back focus d_{BF} , which is the distance of the focal plane from the primary mirror,

$$d_{\text{BF}} = d_2 + d_1. \quad (4)$$

It is more convenient to give three parameters as the focal length of the primary mirror f_1 , the composite focal length f_{comp} , and the focal position, which is usually represented by d_{BF} . Instead of f_1 and f_{comp} , we also use the F -ratio of the primary, $F_1 = f_1/\mathcal{D}_1$, and the composite F -ratio, $F_{\text{comp}} = f_{\text{comp}}/\mathcal{D}_1$. When F_1 , F_{comp} , d_{BF} , and the diameter of the primary \mathcal{D}_1 are given as design parameters, f_1 , f_{comp} , r_1 , d_1 , and r_2 are derived by

$$f_1 = F_1 \mathcal{D}_1, \quad (5)$$

$$f_{\text{comp}} = f_1 \frac{F_{\text{comp}}}{F_1}, \quad (6)$$

$$r_1 = -2f_1, \quad (7)$$

$$d_1 = -f_1 \frac{f_{\text{comp}} - d_{\text{BF}}}{f_{\text{comp}} + f_1}, \quad (8)$$

and

$$r_2 = -2f_{\text{comp}} \frac{f_1 + d_1}{f_{\text{comp}} - f_1}. \quad (9)$$

Besides the radius, a surface has parameters to characterize its figure: the conic constant, k , and the coefficients of higher-order aspheric terms. We describe in the following the design principle of basic two-mirror optics systems characterized by k_1 and k_2 , since the third-order aberration coefficients are governed by these parameters.

In a two-mirror system, because k_1 and k_2 are determined as functions of r_1 , r_2 , and d_1 , the astigmatism C and the curvature of field D are also functions of r_1 , r_2 , and d_1 . Schwarzschild (1905) provided an anastigmat solution with a flat field as $d = 2f$ and $r_1 = 2\sqrt{2}f$, where f is the composite focal length, and is given by $1/f = 2/r_1 + 2/r_2 - 4d/r_1r_2$. Two concentric sphere system with $d_1 = -r_1(1 + \sqrt{5})/2$ also gives an anastigmat solution, known as Schwarzschild optics, which is used in the microscope objective (Burch 1947). However, if the radii and the distance between the mirrors are to be determined by other requirements, such as the final focal ratio and the back focal distance, we can no longer make a two-mirror system anastigmatic.

The classical Cassegrain or Gregorian telescope uses a paraboloid for the primary ($k_1 = -1$) and a hyperboloid for the secondary ($k_2 \neq -1$). This arrangement makes it possible to have a pinpoint image on the optical axis by making the spherical aberration $B = 0$ by appropriately choosing k_2 , but the field of view is limited by remaining non-zero coma F .

A Ritchey–Chrétien telescope has no spherical aberration or coma. The use of hyperboloids for both the primary and secondary makes it possible to vanish two principal aberrations (k_1 and k_2 are used to make $B = F = 0$). Most of the modern large telescopes adopt the Ritchey–Chrétien system because of its wider field of view compared with the classical Cassegrain or Gregorian system.

The remaining aberrations among the third-order aberrations, excepting the distortion, are the astigmatism, C , and the curvature of field, D . With k_1 and k_2 already used to make $B = F = 0$ for the Ritchey–Chrétien system, there are no parameters available to control C and D . It is thus clear that we cannot make an anastigmat with a two-mirror system except for some special cases (Schwarzschild 1905; Burch 1947).

3. Three-Mirror System

In our three-mirror system, the last mirror is placed so that it refocuses the intermediate image made by the first two mirrors. The intermediate focal plane of the first two mirrors is used as a virtual third surface, and the last concave mirror is numbered as the fourth surface.

Three additional free parameters introduced are d_3 , r_4 , and k_4 . We determine r_4 by the condition that the Petzval sum P vanishes,

$$\frac{1}{r_1} - \frac{1}{r_2} + \frac{1}{r_4} = 0. \quad (10)$$

For ordinary telescopes, because the radius of curvature of the primary mirror is larger than that of the secondary mirror, $1/|r_1|$ is smaller than $1/|r_2|$. Therefore, the sign of the sum of the first two terms is determined by r_2 . Therefore, r_2 and r_4 should have the same sign. Since $r_4 < 0$, $r_2 < 0$, the first two-mirror system should be of the Cassegrain type, not of the Gregorian type.

The distance d_4 from the third mirror to the final focal position is calculated by

$$\frac{1}{d_3} + \frac{1}{|d_4|} = \frac{2}{|r_4|}. \quad (11)$$

The magnification factor M by the third mirror is given by

$$M = \left| \frac{d_4}{d_3} \right|. \quad (12)$$

Using k_1 , k_2 , and k_4 , we can make $B = F = C = 0$. When we set $P = 0$, we automatically have $D = 0$. We thus obtained an anastigmatic optical system with a flat focal plane. As for the treatment of higher order aberration and an evaluation of the optical systems, readers might wish to see some reviews (e.g., Wilson 1996; Schroeder 1987). We have not attempted to obtain explicit mathematical expressions for the aberration coefficients of this three-mirror system, but used an optimization procedure provided by the optical design program *optik* written by one of the authors (K.N.). Since the sixth-order aspheric coefficients of the mirror surface affect the fifth-order aberration, the sixth-order aspheric coefficient of the primary mirror is used to control the spherical aberration of the fifth order of the system. For this case, too, we used the optimizing function of *optik*. The mathematical expressions for the fifth-order aberration coefficients can be found, for instance, in Matsui (1972). Because there are 12 independent fifth-order aberrations, it is not as straightforward as in the third-order case to control them with available aspheric coefficients, excepting the case of the fifth-order spherical aberration. We therefore treat only the fifth-order spherical aberration using the sixth-order aspheric coefficient of the primary mirror.

4. Exit Pupil

We now consider the position and the radius of the exit pupil before discussing the vignetting problem. Let us study the size of the radius of the exit pupil first. We take the primary mirror as the pupil.

We write the lens equations for the second and third mirrors with the sign convention for a single mirror; namely, f_2 is negative since the mirror is convex and f_4 is positive since the mirror is concave. Let t_i and t'_i be the distances that appear in the imaging of pupil by the i -th lens. Note that t_2 and t_4 are positive, whereas t'_2 is negative, since the image is imaginary and t'_4 is positive, since the image is real.

The lens equation for the second mirror and the third mirror (= surface 4) is written as

$$\frac{1}{t_i} + \frac{1}{t'_i} = \frac{1}{f_i}, \quad (i = 2, 4). \quad (13)$$

Let us define ξ_i and η_i as

$$\xi_i = \frac{f_i}{t_i}, \quad \eta_i = \frac{t'_i}{t_i}, \quad (i = 2, 4). \quad (14)$$

Then, η_i can be rewritten with ξ_i or with f_i and t_i as

$$\eta_i = \frac{\xi_i}{1 - \xi_i} = \frac{f_i}{t_i - f_i}, \quad (i = 2, 4). \quad (15)$$

Since the distance between the first and the second mirror is usually large compared to the focal length of the secondary mirror, ξ_2 and η_2 are small compared to unity, say, 0.1 in a typical case. If the center of curvature of the third mirror is placed at the focal position of the first two mirrors, $f_4 = d_4/2$ and ξ_4 and η_4 may have a value of around 0.3. Using

$$t_2 = d_1, \quad t_4 = d_2 + d_3 - t'_2 = d_2 + d_3 - f_2(1 + \eta_2), \quad (16)$$

we can rewrite equation (14) explicitly as

$$\xi_2 = \frac{f_2}{d_1}, \quad \xi_4 = \frac{f_4}{d_2 + d_3 - t'_2} = \frac{f_4}{d_2 + d_3 - \frac{d_1 f_2}{d_1 - f_2}}, \quad (17)$$

$$\eta_2 = \frac{f_2}{d_1 - f_2}, \quad \eta_4 = \frac{f_4}{d_2 + d_3 - \frac{d_1 f_2}{d_1 - f_2} - f_4}. \quad (18)$$

The radius R_{ep} of the exit pupil is the radius of the entrance pupil, $\mathcal{D}_1/2$, multiplied by t'_2/t_2 and t'_4/t_4 ,

$$R_{\text{ep}} = \frac{\mathcal{D}_1}{2} \frac{t'_2}{t_2} \frac{t'_4}{t_4} = \frac{\mathcal{D}_1 \eta_2 \eta_4}{2} \quad (19)$$

$$= \frac{\mathcal{D}_1}{2} \frac{f_2}{(d_1 - f_2)} \frac{f_4}{\left(d_2 + d_3 - \frac{d_1 f_2}{d_1 - f_2} - f_4\right)}. \quad (20)$$

The position of the exit pupil is written as

$$t'_4 = \frac{f_4}{1 - \xi_4} = f_4(1 + \eta_4). \quad (21)$$

Note that the current optical system is not telecentric, since the exit pupil is at a finite distance. The principal rays in the final focal plane are not collimated, but are diverging in proportion to the distance from the optical axis. This feature, however, will not be a practical difficulty in designing the observational instrument, unless one wants to cover the entire field, filling 2m in diameter, in a single optical train.

Table 1. Coordinates of a few key points for the vignetting geometry.

Point	z	x	Surface	Description
H _V	$-d_3$	h	3	light enters here
H _P	$-t'_4$	R_{ep}	5	upper edge of the exit pupil
H _F	$-d_4$	$-Mh$	6	light images here

5. Obstruction

5.1. Obstruction when $M > 1$

The detector unit at the final focal plane obstructs the ray bundle that goes through the intermediate focal plane of the first two-mirror system. We solve this problem by using only the semi-circular half field of view at the focal plane of the first two mirrors. If the magnification is $M = 1$, the image on one half field at this virtual plane is reimaged to the other half side, where the detector can be placed without essential vignetting.

If the magnification/minification factor, M , is not unity, the field of view without vignetting is narrowed because of obstruction. It is easy to see that obstruction on the optical axis is always 50% regardless of the value of M .

Figure 1 illustrates the geometry, showing the third mirror, pupil plane, virtual image plane, and final image plane, where the position along the optical axis (z -axis) of each surface is measured from the origin set at the apex of the third mirror. In figure 1, we assume that at the virtual focal plane of the two-mirror system (surface 3), light passes from left to right above the axis ($x > 0$), reflected at the third mirror (surface 4), passing through the exit pupil (surface 5), and imaged at the final focal plane below the optical axis ($x < 0$) (surface 6).

The point A($-d_3, 0$) at the field center of the virtual image plane is reimaged by the third mirror onto the point B($-d_4, 0$) of the final image plane. The upper half of the beam from point A is vignetted at the folding mirror, and does not reach to point B on the detector surface. The limiting radius, h , on the virtual image plane, beyond which the beam from the virtual plane is reflected by the third mirror and refocused on the detector surface, does not suffer any obstruction, and is defined by joining the edge point, A, of the folding mirror and the edge point H_P($-t'_4, R_{\text{ep}}$), of the exit pupil.

Table 1 gives the coordinates of some particular points for defining the edge of the partially vignetted field.

Because $\triangle BH_{\text{F}}A$ and $\triangle PH_{\text{P}}A$ are similar to each other,

$$\frac{Mh}{R_{\text{ep}}} = \frac{(M-1)d_3}{d_3 - t'_4}. \quad (22)$$

Thus, the limiting radius on the image plane, Mh , is written as

$$Mh = R_{\text{ep}} \frac{(M-1)d_3}{d_3 - t'_4} \quad (23)$$

$$= R_{\text{ep}}(M-1) \frac{1}{1 - \frac{t'_4}{d_3}} = \frac{R_{\text{ep}}(M^2 - 1)}{1 - M\eta_4}. \quad (24)$$

5.2. Obstruction when $M < 1$

In this case, the final image plane is closer to the third mirror than is the virtual image plane, as shown in figure 2.

Because $\triangle BH_V A$ and $\triangle PH_P B$ are similar to each other,

$$\frac{h}{R_{\text{ep}}} = \frac{(1-M)d_3}{Md_3 - t'_4}. \quad (25)$$

Thus, the limiting radius on the image plane, Mh , is written as

$$Mh = R_{\text{ep}} M \frac{(1-M)d_3}{Md_3 - t'_4} \quad (26)$$

$$= R_{\text{ep}}(1-M) \frac{1}{1 - \frac{t'_4}{Md_3}} = \frac{R_{\text{ep}}(1-M^2)}{M - \eta_4}. \quad (27)$$

5.3. Limiting Radius for the Vignetting-Free Field

Because the 1 arcminute on the image plane is

$$a = f_{\text{comp}} \frac{\pi}{180 \times 60} = F_{\text{comp}} \mathcal{D}_1 \frac{\pi}{180 \times 60}, \quad (28)$$

the limiting radius, Mh , in arcminute scale, a , is expressed as

$$\frac{R_{\text{ep}}(M^2 - 1)}{1 - M\eta_4} \frac{1}{a} = \frac{1}{2F_{\text{comp}}} \frac{M^2 - 1}{1 - M\eta_4} \eta_2 \eta_4 \frac{180 \times 60}{\pi} \quad (M > 1) \quad (29)$$

and

$$\frac{R_{\text{ep}}(1 - M^2)}{M - \eta_4} \frac{1}{a} = \frac{1}{2F_{\text{comp}}} \frac{1 - M^2}{M - \eta_4} \eta_2 \eta_4 \frac{180 \times 60}{\pi} \quad (1 > M). \quad (30)$$

In a typical case, if we take the radius of field of view as $6'$ and allow $1'$ to be the limiting radius for the vignetting-free field, we have

$$0.9 < M < 1.1. \quad (31)$$

Figure 3 shows the optical throughput of the present system for three cases with $M = 1.0$, 0.9 , and 0.8 . Note that for $M = 1$, the 50% vignetting takes place only along the $x = 0$ axis of the semi-circular field. The field away from this axis by the diffraction size of the optics can be made essentially obstruction-free.

6. Example Layout to Cover the Circular Field

Figure 4 shows an example layout of an all-mirror anastigmat telescope to cover a full circular field of view of $10'$ radius by two optical branches, each covering a semi-circular field of view. In this figure, only one of the two optical branches is shown, for simplicity. By folding the beam by flat mirrors, M3 and M4, one can have an unvignetted semi-circular focal plane FP reimaged by M5 (third aspheric mirror), and refolded by M6 as shown in figure 5, where two optical branches are shown. Table 2 gives the lens data of the optical system shown in figure 4.

A spot diagram out to $10'$ from the optical axis is shown in figure 6. Note that the designed spot sizes are smaller than the diffraction circle for a 30 m ELT out to $8'$.

Actual manufacturing of such an anastigmat system needs to be further studied.

7. Conclusion

The present three-mirror anastigmat telescope system provides a flat focal plane with diffraction-limited imaging capability with minimal vignetting. The magnification factor by the third mirror, M , should be designed to be close to unity. Although only a semi-circular field of view can be made unvignetted in one optical train, one can cover the entire circular field without vignetting by deploying two such separate optical trains, each covering a semi-circular field.

The present system is similar to the three-mirror anastigmat Korsch system with a 45° mirror placed at the pupil plane (Korsch 1980) concerning its aberration-free optical performance. However, the magnification factor by the third mirror, M , should be large in order to make the vignetting factor small for the Korsch system, whereas the magnification factor by the third mirror should be close to unity in the present system. Therefore, the present system can be used for applications that require a wider field of view. Another merit of the present system is the avoidance of central obscuration.

The authors are grateful to Dr. A. Rakich, who kindly pointed out the existence of many important classical and modern papers to be referred in relation to the three-mirror telescope design. They also appreciate comments of Dr. Y. Yamashita on the background of the present work.

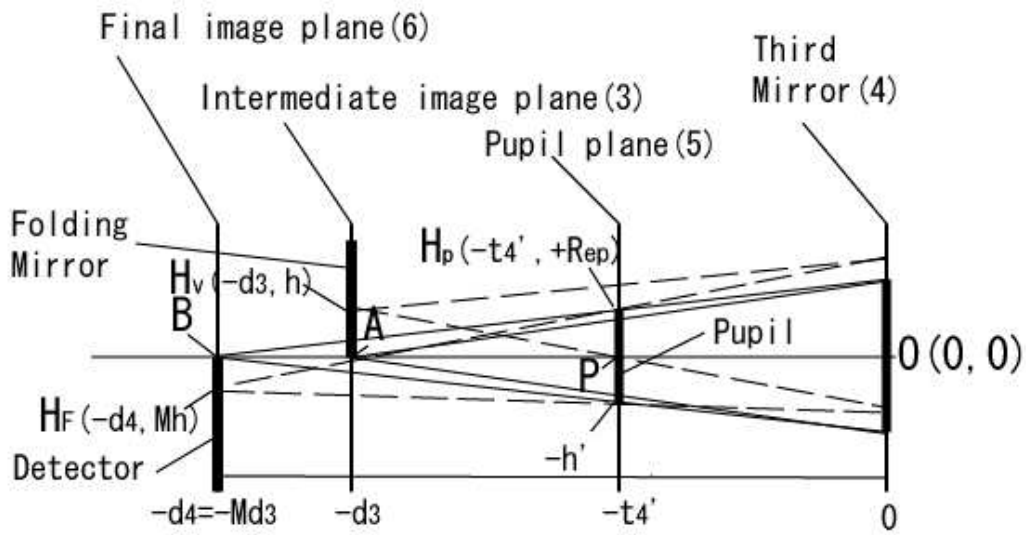


Fig. 1. Geometry of rays defining the vignetting field for $M > 1$.

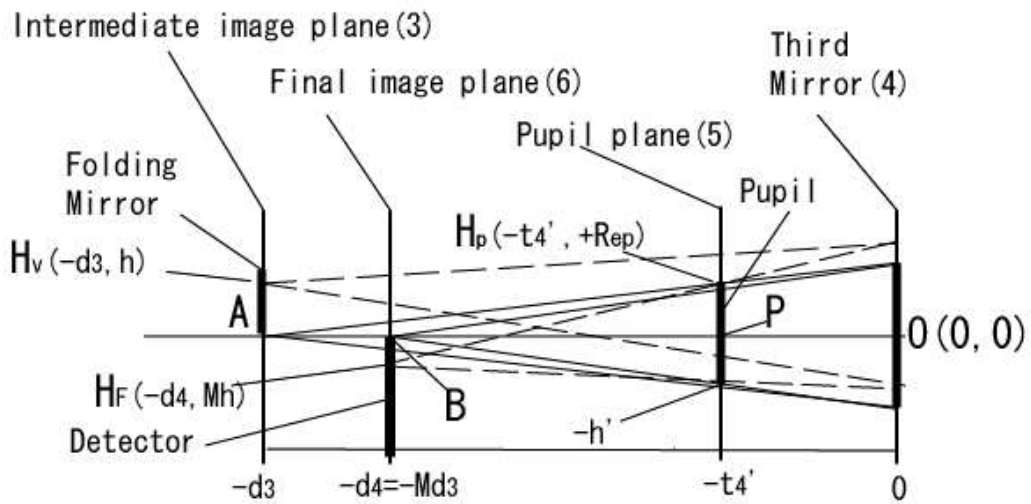


Fig. 2. Geometry of rays defining the vignetting field for $M < 1$.

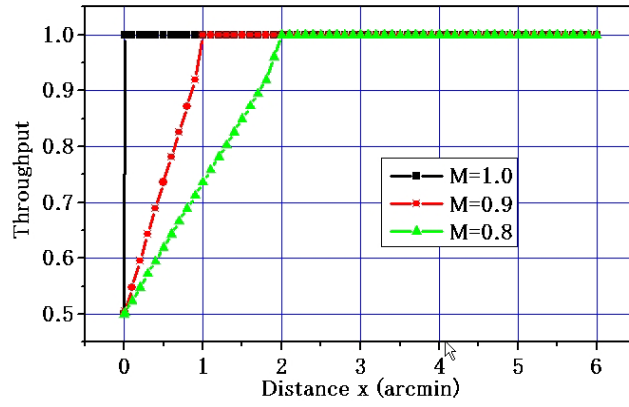


Fig. 3. Optical throughput due to geometrical obstruction for $M = 1, 0.9,$ and 0.8 .

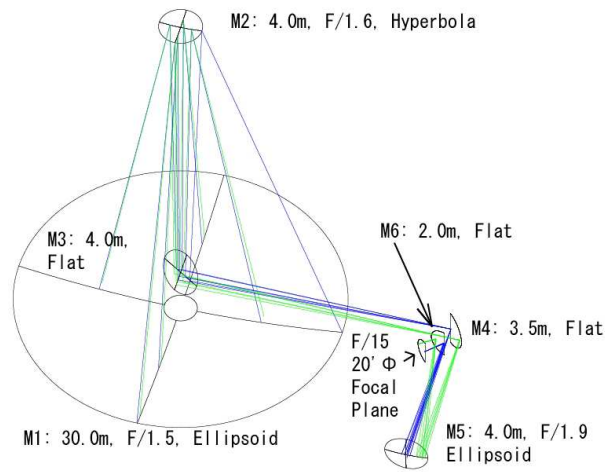


Fig. 4. Example optical layout for a three aspheric mirror system.

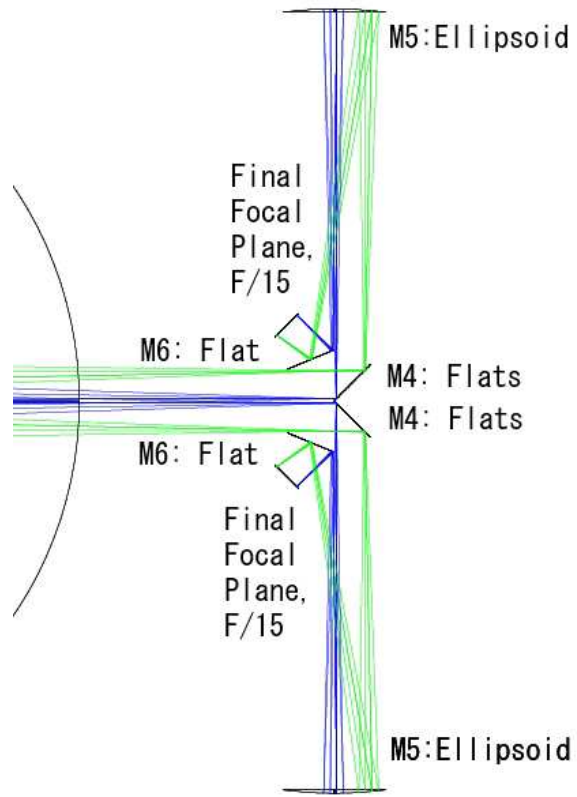


Fig. 5. Example layout to avoid field vignetting and securing space to deploy observational instruments.

Table 2. Preliminary lens data for the 30m JELT.

Number	Surface type	Radius	Thickness	Glass	Distance	Conic	ϕ_v	ϕ_h	Surface [†]
OBJ	Standard	1.0E+040	Infinity		Infinity	0.0			
1*	Even Asphere	-90.0	-39.090909	Mirror M1	15.0	-0.992036	1.5E-015	0.0	
STOP	Even Asphere	-13.131313	34.090909	Mirror M2	1.975613	-1.412689	0.0	0.0	
3	Coord Break		0.0	...	0.0		45.0	0.0	
4*	Standard	1.0E+040	0.0	Mirror M3	2.112906	0.0			
5	Coord Break		-25.0	...	0.0		45.0	0.0	
6	Coord Break		0.0	...	0.0		0.0	45.0	
7*	Standard	1.0E+040	0.0	Mirror M4	1.772806	0.0			3
8	Coord Break		15.374510	...	0.0		0.0	45.0	
9*	Even Asphere	-15.374510	-13.374510	Mirror M5	1.999334	-0.720989	0.0	0.0	4
10	Coord Break		0.0	...	0.0		0.0	-22.5	
11*	Standard	1.0E+040	0.0	Mirror M6	1.039940	0.0			6
12	Coord Break		2.0	...	0.0		0.0	-22.5	
IMA	-1.0E+040			1.185943	0.0				

ϕ_v denotes the angle of folding flat mirror to redirect the optical axis within the vertical plane.

ϕ_h denotes the angle of folding flat mirror to redirect the optical axis within the horizontal plane.

* denotes physical surfaces.

† denotes the surface number corresponding to those referred in subsection 5.1 and figures 1 and 2.

References

- Burch, C. R. 1947, Proc. Phys. Soc., 59, 41
- Epps, H. W., & Takeda, M. 1983, Ann. Tokyo Astron. Obs., 19, 401
- Korsch, D. 1980, Appl. Opt. 19, 3640
- Matsui, Y. 1972, Lens Sekkeiho (Tokyo: Kyoritu Publishing Co.),
in Japanese
- Meinel, A. B., Meinel, M. P., Su, D.-Q., & Wang, Y.-N. 1984, Appl. Opt., 23, 3020
- Paul, M. 1935, Rev. Opt., A14, 169
- Rakich, A. 2002, Proc. SPIE, 4768, 32
- Rakich, A., & Rumsey, N. 2002, J. Opt. Soc. Am. A, 19, 1398
- Rakich, A., & Rumsey, N. J. 2004, Proc. SPIE, 5249, 103
- Robb, P. N. 1978, Appl. Opt., 17, 2677
- Schroeder, D. J. 1987, Astronomical Optics (New York: Academic Press)
- Schwarzschild, K. 1905, Investigations into Geometrical Optics II, Theory of Mirror Telescopes, English translation by A. Rakich, (<http://members.iinet.net.au/~arakich/>)
- Willstrop, R. V. 1984, MNRAS, 210, 597

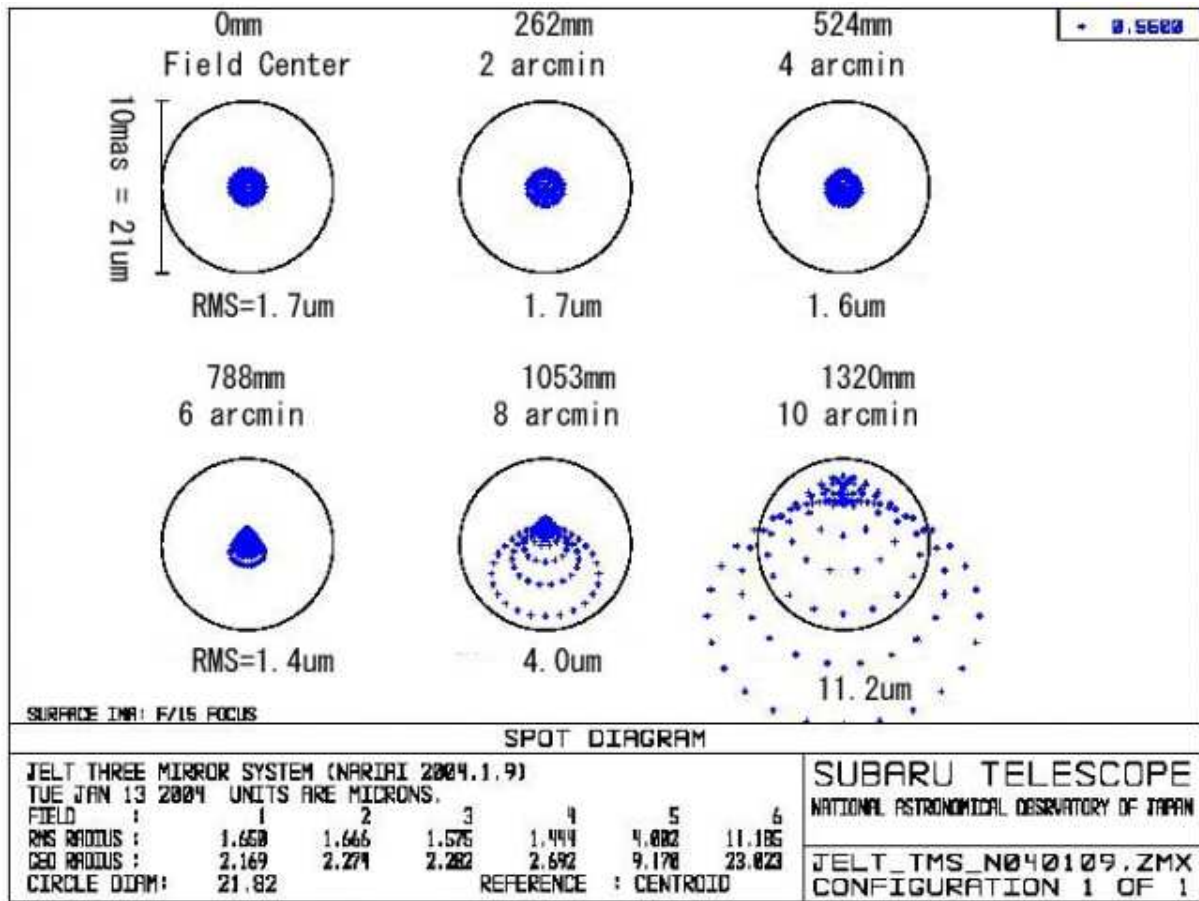


Fig. 6. Spot diagrams up to a 10' radius field.

Willstrop, R. V. 1985, MNRAS, 216, 411

Wilson, R. N. 1996, Reflecting Telescope Optics I, Basic Design Theory and its Historical Development (Berlin: Springer-Verlag)

Wilson, R. N., Delabre, B., & Franza, F. 1994, Proc. SPIE, 2199, 1052

Yamashita, Y., & Nariai, K. 1983, Ann. Tokyo Astron. Obs., 19, 375